A methodology for optimisation design and analysis of stratosphere airship

Q. Wang, J. Chen, G. Fu, D. Duan and H. Zhao
Institute of Aerospace Science & Technology
Shanghai Jiaotong University
Shanghai, China

ABSTRACT

This paper presents a methodology for studying the feasibility of stratosphere airship for high altitude long endurance missions and arriving at the baseline specifications of conventional configuration of stratosphere airship, given the performance and operational requirements. Based on this methodology, the AODAP platform (Airship Optimisation Design and Analysis Platform) was developed. Some innovative concepts used in AODAP that are different from previous methods and codes are presented. The shape optimisation of airship was introduced into the design process, and several optimum objectives can be selected including minimum drag, minimum weight and composite objective based on MDO (Multidisciplinary Design Optimisation). The methodology was validated for other design concepts previously developed for similar missions and also was compared to a low altitude vehicle. The baseline specifications of stratosphere airships designed for various shapes using this methodology are presented. The results of sensitivity analyses for a specified airship are discussed, and the sensitivity of airship length with some critical parameters including area density of envelope fabric, area density of solar cell, efficiency of solar cell and efficiency of fuel cell for the specified shape is also provided.

NOMENCLATURE

A_{sa}	surface area of solar array
A_{saF}	initiation value of A_{sa}
A_e	surface area of envelope
A_{eF}	initiation value of A_e
a, b, c, d	shape coefficients of airship
C_{DV}	coefficient of volumetric drag
C_{DVF}	initiation value of C_{DV}
D	maximum diameter of envelope
F_{drag}	drag force
F_{prop}	propulsion force
g	acceleration of gravity
I_b	solar radiation perpendicular to the surface
I_n	intensity of the solar radiation
$\mathbf{l}_{\mathbf{sun}}$	transformed normal vector of solar radiation
$\mathbf{l}_{\mathbf{sunO}}$	normal vector of solar radiation
$\mathbf{n}$	normal vector of the surface
P	vector of the surface
p	power
p_{static}	static pressure
p_{dyn}	Munk pressure

Paper No. 3435. Manuscript received 23 March 2009, revised 12 May 2009, accepted 29 May 2009.

https://doi.org/10.1017/S0001924000003183 Published online by Cambridge University Press

p_{diff}	internal differential pressure
Q_{total}	total energy required
Q_{sc}	total energy generated by solar cell
Re	Reynold's number
r	radius
$\mathbf{T_m}$	a transformation matrix
t_{allday}	twenty-four-hour period
t_{day}	period from sunrise to sunset
t_{night}	period from sunset to sunrise
V	volume
v	velocity
x	X-location
ΔP	minimum internal overpressure
α	sun azimuth angle
β	sun elevation angle
γ	angle along the circumference
δ	judgment factor
η_{fc}	efficiency of fuel cell
η_{prop}	efficiency of propulsion systems
η_{sc}	efficiency of solar cell
μ	dynamic viscosity of air
ρ	density of air
σ_{min}	minimum hoop stress
σ_{minF}	initiation value of smin
Θ	airship pitch angle
Φ	airship roll angle
Ψ	airship yaw angle (0° for east, 270° for north)

Subscripts

bc	buoyancy centre
ctrls	control system gc gravity centre
pays	payload system
props	propulsion system

1.0 INTRODUCTION

In general, there are three phases in typical aircraft design, namely, conceptual, preliminary, and detailed design. Of the three phases, the conceptual design is the least in terms of the total duration and investment; which is approximate 5% of the total. However, the decision made during this phrase has a direct influence on the effort and cost in the following phases, and the investment decided during this phrase accounts for almost 70% of the total. One of the most important activities in the conceptual design is to arrive at the baseline specifications of an aircraft in order to provide guidance for the final design of the aircraft. Sensitivity analyses which identify the leverage of various design variables on the availability and performance are also an important part of the conceptual design.

Stratosphere airships have been attracting increasing attention for decades, for aerial exploration, environmental monitoring, and surveillance purposes[1]. So far, several methodologies and codes for designing and analysing of airship are available, such as Ozoroski[2] for developing the ADAC code (Airship Design and Analysis Code) and Pant[3] for presenting a methodology for arriving at the baseline specifications of a non-rigid airship. Ozoroski developed the code to study the feasibility of lighter-than-air vehicles designed for high altitude long endurance missions. Pant developed the methodology for a non-rigid airship which is not for high altitude missions. However, neither of them considered the optimisation of the whole procedure of conceptual design. The sensitivities of the critical parameters such as fabric area density of envelope, area density of solar cell, efficiency of solar cell and efficiency of fuel cell are also not mentioned in their studies.

This paper develops a novel methodology to carry out the conceptual design of stratosphere airship as compared to the conventional approaches. We introduce the optimisation into the procedure of design and present a methodology for studying the feasibility of stratosphere airship for high altitude long endurance missions and arriving at the baseline specifications of conventional configuration of stratosphere airship, given the design requirements. The ADOAP platform was also developed based on the methodology. The sensitivity of airship length with some critical parameters for specified shape is also given and the results of sensitivity analyses are presented.

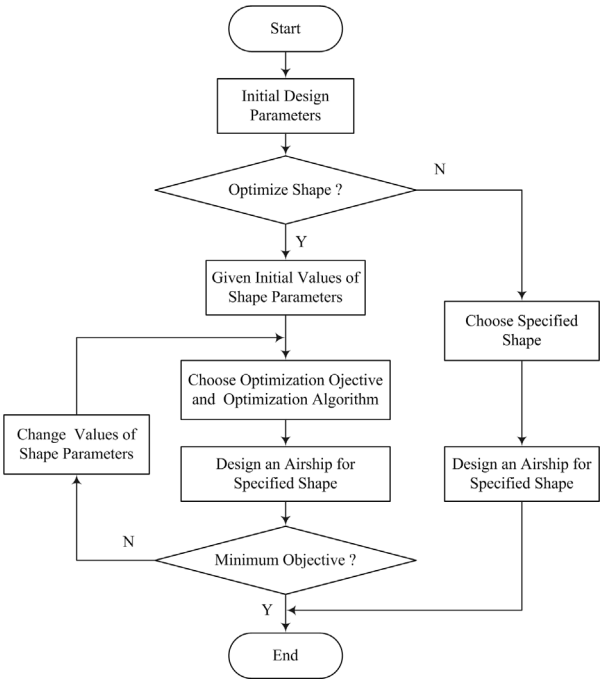


Figure 1. Flow chart of the methodology.

2.0 OUTLINE OF THE METHODOLOGY

The flow chart of the methodology is shown in Fig. 1. The calculations are initiated with the predefined values of input parameters. The values of the parameters can be modified according to the design conditions and requirements. When the input parameters are set, the shape type should be defined by choosing specified option of shape type.

If the option of 'Optimum Shape' is chosen, then the initial values of shape parameters are given. Then the inner loop titled 'Design an Airship for Specified Shape' is executed to find the minimum length of airship for given shape and design conditions. If the design results meet the requirement of optimisation, the optimisation procedure is stopped and the design results are obtained. Otherwise, the values of shape parameters are changed for the next loop until the results are acceptable. The whole procedure of optimisation is performed using optimisation algorithm chosen by the users.

If the option of 'Optimum Shape' is not chosen, the specified shape existed in the program should be defined. Then the inner loop is executed to determined the minimum airship length meeting the design requirement for given shape and provide the corresponding design results.

The flow chart of the inner loop titled 'Design an Airship for Specified Shape' in Fig. 1 is showed in Fig. 2. The initial length is large enough so that it can avoid making mistakes due to a shortage of airship size in the process of calculation. The next step is the calculation of geometric parameters of the airship, which include the dimensions of the envelope, ballonets, the fins, the cones and the

https://doi.org/10.1017/S0001924000003183 Published online by Cambridge University Press

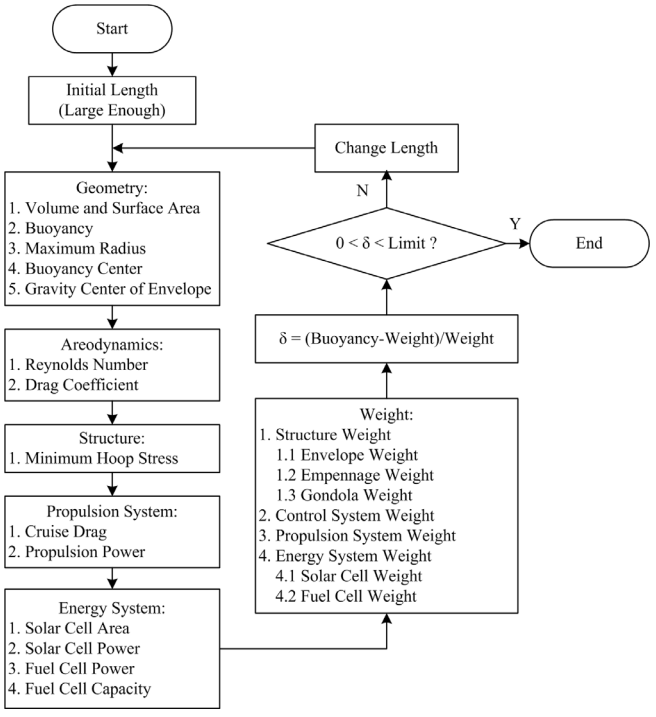


Figure 2. Flow chart of 'Design an Airship for Specified Shape'.

gondola. This is followed by the calculation of aerodynamics parameters including Reynolds number, drag coefficient and cruise drag. In the step of structure system design, the minimum hoop stress is calculated to make sure the safety of the envelope and ballonet. The next step is the design of energy system, in which the solar cell power, the solar cell area, the fuel cell power and the fuel cell capacity are provided. The last step is the calculation of weight breakdown of various components and hence the empty weight.

The factor δ in Fig. 2 is adopted to make sure that the final result not only meets the requirement of the minimum dimensions but also makes sure the validation of the design. Whether this design loop is valid or not is determined by the comparison between the factor and a given limit. If the factor does not match the limit, then airship length is adjusted and the calculation is repeated. The process is stopped when the value of the factor meets the requirement of the criteria.

For the given shape of an airship, the sensitivity analyses of design parameters can be executed only using the inner loop.

3.0 KEY SUB-MODULES OF THE METHODOLOGY

A description of the key sub-modules of the methodology is given as follows.

3.1 Atmospheric model

The atmospheric model used is the Standard Model Atmosphere[4]. Once a mission altitude is determined, the program automatically calculates the corresponding temperature, pressure and density for that altitude.

3.2 Shape generation algorithm

To explore the possibility of better shapes in view of the multidisciplinary optimisation characteristics, a new shape generation algorithm was proposed to extend the range of design space. The

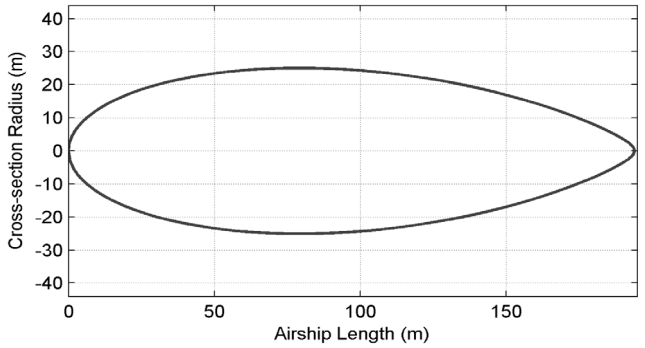


Figure 3. Default shape.

equation of the airship body is expressed as follows:

$$64(y^2+z^2)=a(l-x)(bx-l\sqrt{c}+\sqrt{cl^2-dlx}) \quad \ldots (1)$$

Since the complete airship body is obtained by revolving the 2D shape by 360° about the X-axis, the 2D shape equation can be transformed as follows:

$$y=\frac{1}{8}\sqrt{a(l-x)(bx-l\sqrt{c}+\sqrt{cl^2-dlx})} \quad \ldots (2)$$

The default shape is shown in Fig. 3.

3.3 Model of geometry

The volume of the envelope (V_e) can be calculated as follows:

$$V_e=\pi\int_0^a y^2\mathrm{d}x \quad \ldots (3)$$

The surface area of the envelope (A_e) can be obtained as follows:

$$A_e=2\pi\int_0^a y\cdot\left(1+\left(\frac{\mathrm{d}y}{\mathrm{d}x}\right)^2\right)^{\frac{1}{2}}\mathrm{d}x \quad \ldots (4)$$

The X location of centre of buoyancy (x_{bc}) is depicted as

$$A_e=2\pi\int_0^a y\cdot\left(1+\left(\frac{\mathrm{d}y}{\mathrm{d}x}\right)^2\right)^{\frac{1}{2}}\mathrm{d}x \quad \ldots (5)$$

The X location of centre of the envelope gravity (x_{gc}) is depicted as

$$x_{gc}=2\pi\int_0^a x\cdot y\cdot\left(1+\left(\frac{\mathrm{d}y}{\mathrm{d}x}\right)^2\right)^{\frac{1}{2}}\mathrm{d}x\Big/A_e \quad \ldots (6)$$

The X location of maximum diameter of the envelope can be calculated with the first derivative of y in Equation (2) as follows:

$$y'=\frac{\mathrm{d}y}{\mathrm{d}x}=0 \quad \ldots (7)$$

Then the maximum diameter can be obtained with the X location of maximum diameter based on Equation (2).

3.4 Model of volumetric drag coefficient

The volumetric coefficient of drag (C_{DV}) which is calculated based on $V^{2/3}$ has been given by Khoury and Gillet[5] as a function of fineness ratio (l/D) and is described as follows:

https://doi.org/10.1017/S0001924000003183 Published online by Cambridge University Press

$$C_{DV} = \frac{0\cdot172(l/D)^{1/3} + 0\cdot252(D/l)^{1\cdot2} + 1\cdot032(D/l)^{2\cdot7}}{\mathrm{Re}^{1/6}} \quad \ldots (8)$$

$$\mathrm{Re} = \frac{\rho_a v l}{\mu} \quad \ldots (9)$$

3.5 Model of minimum hoop stress

The minimum hoop stress per unit thickness is obtained by Equation (10). The minimum inner pressure (ΔP) in the Equation (10) consisting of static pressure (p_{static}), Munk Pressure (p_{dyn}) and the internal differential pressure (p_{diff}) is depicted in Equation (11). Static pressure caused by static bending moments, Munk pressure due to the dynamic bending moments and the internal differential pressure are calculated using Equation (12), Equation (13) and Equation (14) respectively.

$$\sigma_{min} = \Delta P D/2 \quad \ldots (10)$$

$$\Delta P = p_{static} + p_{dyn} + p_{diff} \quad \ldots (11)$$

$$p_{static} = 0\cdot2308 g \rho_a r_{gc} \lambda^2 \quad \ldots (12)$$

$$p_{dyn} = \rho_a v^2 V_e \left(k_2 - k_1\right) \mathrm{Sin}2\alpha / (\pi r_{gc}^3) \quad \ldots (13)$$

$$p_{diff} = 1\cdot722 g \rho_a R \lambda \mathrm{Sin}\alpha \quad \ldots (14)$$

3.6 Model of propulsion power

The power used for propulsion can be calculated as

$$p_{props} = F_{prop} v / \eta_{prop} \quad \ldots (15)$$

where

$$F_{prop} = F_{drag} \quad \ldots (16)$$

$$F_{drag} = \frac{1}{2} \rho_a v^2 C_{DV} V_e^{2/3} \quad \ldots (17)$$

3.7 Model of energy system

The power required to run an airship and its payloads consists mostly of control system (p_{ctrls}), payload system (p_{pays}) and propulsion system (p_{props}). Of these, the propulsion system uses by far the greatest amount of energy. Around 100kW of propulsion power is required when flying at 25ms^{-1}. The payload systems use around 10kW and the control system about 11kW[6], both of which can be assumed to be constant during design. The total power required can be described as follows:

$$p_{total} = p_{pays} + p_{ctrls} + p_{props} \quad \ldots (18)$$

For long endurance missions, the energy is obtained mostly using solar powered regenerative fuel cells and only part of the collected solar irradiance is available for the direct propulsion and the rest has to be used to charge the energy storage for the night time. The sketch of energy system is showed in Fig. 4.

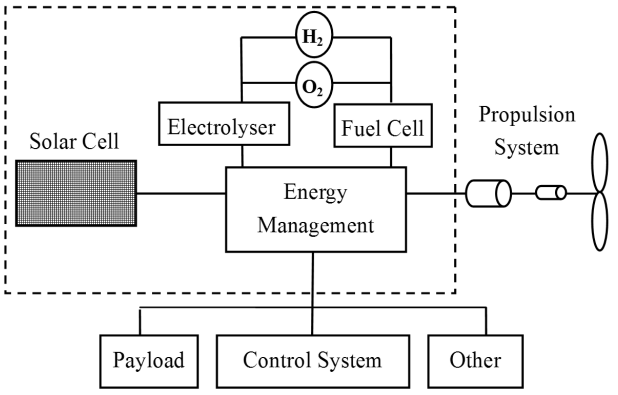


Figure 4. Energy system configuration sketch.

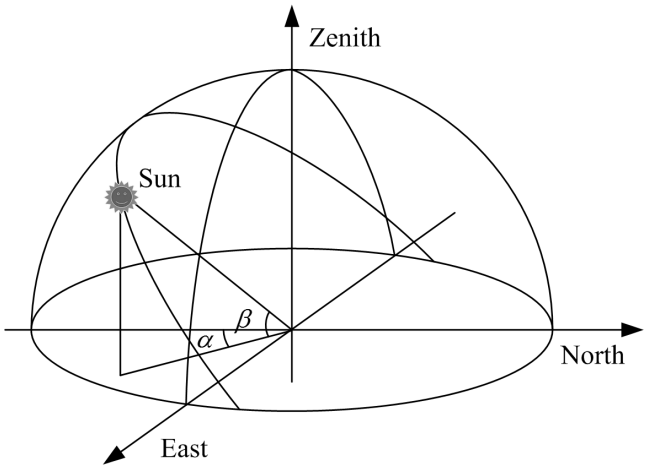


Figure 5. Sketch of sun angles.

The total energy required is depicted as

$$Q_{total} = p_{total} t_{day} + p_{total} t_{night} / \eta_{fc} \quad \ldots (19)$$

$$t_{night} = t_{allday} - t_{day} \quad \ldots (20)$$

For the purpose of calculating the area of the solar array, the shape of the airship can be assumed approximately as a cylinder. The radius of the envelope at the mass centre (r_{gc}) is adopted as the radius of the cylinder. Thus a vector which defines any point on the surface can be created as a function of the radius of a cylinder (r_{gc}), location (x) and angle along the circumference (γ), and is given by

$$P(x, y, z) = (x, r_{gc}\mathrm{Sin}\gamma, r_{gc}\mathrm{Cos}\gamma) \quad \ldots (21)$$

Using Equation (21) the normal vector of the surface is

$$\bar{n}(x, y, z) = (0, \mathrm{Sin}\gamma, \mathrm{Cos}\gamma) \quad \ldots (22)$$

As shown in Fig. 5, the sun elevation angle (β) and the azimuth angle (α) are changing with the time, which determine the direction of the solar incidence ray. The normal vector of solar radiation is

$$\bar{l}_{sunO} = \begin{pmatrix} \mathrm{Sin}\alpha\ \mathrm{Cos}\beta \\ \mathrm{Cos}\alpha\ \mathrm{Cos}\beta \\ \mathrm{Sin}\beta \end{pmatrix} \quad \ldots (23)$$

https://doi.org/10.1017/S0001924000003183 Published online by Cambridge University Press

The solar radiation vector can be resolved into two parts: one perpendicular to the solar array surface and one parallel to it. Of these two parts only the perpendicular one of the solar radiation vector is effective in producing electrical energy. This perpendicular part can be calculated using the dot product of the solar vector and the local normal vector of the solar array surface, providing these two vectors are relative to the same axis system. For this purpose the solar radiation vector is transformed to the local airship axis system by Equation (24).

$$\bar{l}_{sun} = T_m \cdot \bar{l}_{sunO} = T_m \cdot \begin{pmatrix} \mathrm{Sin}\alpha\,\mathrm{Cos}\beta \\ \mathrm{Cos}\alpha\,\mathrm{Cos}\beta \\ \mathrm{Sin}\beta \end{pmatrix} \quad \ldots (24)$$

In Equation (24) $\mathbf{T_m}$ is a transformation matrix, which transforms the vector from the universal axis system to the local airship axis system. The contents of this matrix depend on the attitude and direction of the airship, and are expressed as follows:

$$\mathbf{T_m} = \begin{pmatrix} \mathrm{Cos}\Theta\,\mathrm{Cos}\Psi & \mathrm{Cos}\Theta\,\mathrm{Sin}\Psi & -\mathrm{Sin}\Theta \\ -\mathrm{Cos}\Phi\,\mathrm{Sin}\Psi + \mathrm{Sin}\Phi\,\mathrm{Sin}\Theta\,\mathrm{Cos}\Psi & \mathrm{Cos}\Phi\,\mathrm{Cos}\Psi + \mathrm{Sin}\Phi\,\mathrm{Sin}\Theta\,\mathrm{Sin}\Psi & \mathrm{Sin}\Phi\,\mathrm{Cos}\Theta \\ \mathrm{Sin}\Phi\,\mathrm{Sin}\Psi + \mathrm{Cos}\Phi\,\mathrm{Sin}\Theta\,\mathrm{Cos}\Psi & -\mathrm{Sin}\Phi\,\mathrm{Cos}\Psi + \mathrm{Cos}\Phi\,\mathrm{Sin}\Theta\,\mathrm{Sin}\Psi & \mathrm{Cos}\Phi\,\mathrm{Cos}\Theta \end{pmatrix} \quad \ldots (25)$$

When an airship is flying eastwards without any pitch and roll ($\Theta = 0$, $\Phi = 0$, $\Psi = 0$), the matrix becomes

$$\mathbf{T_m} = \begin{pmatrix} 1 & 0 & 0 \\ 0 & 1 & 0 \\ 0 & 0 & 1 \end{pmatrix} \quad \ldots (26)$$

The solar radiation can be calculated using the dot product of the solar radiation and the normal vector of the surface. But the two vectors must be relative to the same axis system for the dot product. When an airship is flying eastwards without any pitch and roll, the solar radiation perpendicular to the surface (I_b) can be obtained from

$$I_b = I_n \frac{\bar{n} \cdot \bar{l}_{sun}}{|\bar{n}| \cdot |\bar{l}_{sun}|} \quad \ldots (27)$$

The amount of electrical energy generated from an area ds can be calculated as

$$\mathrm{d}W = I_b \cdot \eta_{sc} \cdot \mathrm{d}s \quad \ldots (28)$$

where ds is the product of the length along the x-direction and the length along the circumference

$$\mathrm{d}s = \mathrm{d}x \cdot r_{gc}\,\mathrm{d}\gamma \quad \ldots (29)$$

The total amount of energy received on the solar array is then calculated as follows:

$$Q_{sc} = \int_x \int_\gamma \int_t I_n \frac{\bar{n} \cdot \bar{l}_{sun}}{|\bar{n}| \cdot |\bar{l}_{sun}|} \eta_{sc} r_{gc}\,\mathrm{d}\gamma\mathrm{d}x\mathrm{d}t \quad \ldots (30)$$

For the airship to work properly, the energy should satisfy

$$Q_{sc} = Q_{total} \quad \ldots (31)$$

The surface area of the solar array can be obtained easily by Equation (19), Equation (30) and Equation (31) with numerical method, and the area is described as

$$A_{sa} = \int_x \int_\gamma r_{gc}\,\mathrm{d}x\mathrm{d}\gamma \quad \ldots (32)$$

Table 1
Input parameters

User parameters`
Mission altitude
Mission location (latitude and longitude)
Mission payload (weight and power)
Mission time (start and end date)
Max design speed
Cruising speed

Design types
Empennage type
Fin layout type (cross or plus)
Engine type
Fuel cell type
Shape type
Optimisation objective type
Area density of empennage
Fabric factor of safety
Area density of solar cell
Density of fuel cell
Suspension factor
Nose structure factor
Tail structure factor
Propulsion system factor
Control system factor
Other factor

Energy
Efficiency of fuel cell
Efficiency of solar cell
Efficiency of electrical conversion

Design parameters
Weight
Fabric tensile strength of envelope
Area density of envelope fabric
Fabric tensile strength of helium ballonet
Area density of helium ballonet fabric
Efficiency of transmission system
Area safety factor of solar cell

Other
Air percentage

4.0 OPTIMISATION OPTIONS

In this methodology, various optimisation objectives can be chosen with respect to specific design target. The optimisation algorithms can also be selected in terms of accuracy and efficiency for various optimisation objectives.

4.1 Optimisation objectives

Several optimum objectives can be selected including minimum drag, minimum weight and composite objective based on MDO.

The composite objective function involving C_{DV}, A_e, σ_{min}, and A_{sa} was formed as

$$F_{composite} = \frac{1}{4} \times \left(\frac{C_{DV}}{C_{DVF}} + \frac{A_e}{A_{eF}} + \frac{\sigma_{\min}}{\sigma_{\min F}} + \frac{A_{sa}}{A_{saF}} \right) \times 100 \quad \ldots (33)$$

C_{DVF}, A_{eF}, σ_{minF}, and A_{saF} are the respective initiation value of C_{DV}, A_e, σ_{min}, and A_{sa} corresponding to reference shape. The reference shape is used to compare with the shape of the optimised design obtained with this methodology in terms of the composite objective.

4.2 Optimisation algorithms

The methodology adopts several optimisation algorithms for the optimisation of design, including ASA[7], NSGA-II[8] and NLPQL[9], etc. The users can choose the algorithm using point-and-click input interface easily.

5.0 INPUT AND OUTPUT PARAMETERS OF THE METHODOLOGY

The input and output parameters of the methodology are listed in Table 1 and Table 2.

https://doi.org/10.1017/S0001924000003183 Published online by Cambridge University Press

Table 2
Output parameters

Weight	**Geometry**
Structure weight	Volume
Fabric	Surface area of envelope
Empennage	Shape parameters
Nose structure	Buoyancy centre
Tail structure	Gravity centre
Suspension	Max radius
Other	*X*-location of max radius
Energy weight	
Fuel tank	**Power**
Fuel cell	Max power requirement
Solar cell	Control system requirement
Batteries	Payload power requirement
Propulsion system weight	Total power requirement
Control system weight	Solar cell area
Payload weight	
Total weight	**Other**
	Coefficient of drag
	Total buoyancy

Table 3
Comparison between HALE and AODAP predictions

		HALE	AODAP
Altitude		20,000m	20,000m
Length		203m	206m
Volume		181,200.00m^3	188,651.68m^3
Envelope area		20,750m^2	21,446m^2
Max design speed		25ms^{-1}	25ms^{-1}
Weight of payload		500kg	500kg
Power of payload		5kW	5kW
Weight	Structure	62·19%	63·38%
	Energy	28·37 %	28·64%
Breakdown	Other	5·86 %	4·45%
	Payload	3·58 %	3·53%
Total weight		13,968kg	14,176kg

6.0 VALIDATION

The methodology has been validated against the HALE airship[10], the Lockheed HI-SPOT design concept[11] and the Goodyear Blimp GZ-20[12].

HALE is also designed for stratospheric purpose. The detailed list of comparison result is shown in Table 3.

The overall weight breakdown, total weight and size show reasonable agreement with the HALE design.

The HI-SPOT (High altitude Surveillance Platform for Over-the-horizon Targeting) concept design was submitted to the US Navy. This mission is developed to meet the similar requirements of the HAULE (high-altitude ultra-long endurance) mission. The HI-SPOT, which is a 142,000m^3 liquid hydrogen-fueled vehicle, was designed for an optimum altitude of 19km. Table 4 shows the comparison of the HI-SPOT concept and the AODAP design result.

The AODAP design shows reasonable agreement with the HI-SPOT design. The estimated weights compared well with the quoted values, but the C_D value, height and width differences exist due to difference between the shape of the HI-SPOT and the shape of the AODAP.

The Goodyear Blimp GZ-20 is a low altitude airship commonly used for advertising and public relations. The GZ-20 carries two fuel injected engines, producing 210 horsepower each. The usual cruising speed of the GZ20 is 15·64ms^{-1} in a zero wind condition and all-out top speed is 23·69ms^{-1}. The airship can carry enough fuel to fly for 24 hours. The SFC (specific fuel consumption) of the engines could not be determined, so an initial value of 1kg/kW/hr was adopted based on the guidelines provided by Khoury and Gillet[5]. All other variables were set to default values. A comparison between the values of Goodyear GZ-20 and AODAP is listed in Table 5.

Table 4
Comparison between HI-SPOT concept and AODAP predictions

	HI-SPOT	AODAP
Volume	142,000m^3	142,002m^3
Length	153·6m	154m
Height	46·3m	43·6m
Width	46·3m	43·6m
Gross weight	11,748kg	11,018kg
Fuel weight	3,111kg	3,032.2kg
$CD(S = V2/3)$	0·01575	0·02509
Cone weight	327·7kg	280·5kg
Fin weight	314·6kg	313·6kg
Ballonet	1,224·0kg	1,165·9kg
Fabric weight	3924·9kg	3881·3kg
Fuel tank weight	710·0kg	690·3kg

Table 5
Comparisons between Goodyear Blimp GZ-20 and AODAP predictions

	Goodyear GZ-20	AODAP
Volume	5,740m^2	5,740m^3
Length	58·82m	59m
Height	18·14m	13·72m
Width	16·76m	13·72m
Weight	5,824kg	5,335kg

The AODAP design shows reasonable agreement with the Goodyear Blimp GZ-20. The variance in height, width and weight is likely due to the differences and uncertainties in shape, fabric specific gravity, fabric tensile strength, engine SFC, etc.

7.0 DESIGN RESULTS USING AODAP

A conceptual design to meet the stratospheric mission requirements was performed using AODAP. Three shape types adopted in this design are default shape, optimisation shape with minimum drag and optimisation shape with composite objective. The default shape is one of the specified shapes provided in the platform can be chosen by users directly. A summary of the key input parameters and the design results for various shape types are showed in Table 6. The airship shapes of these conceptual designs are showed in Fig. 6.

8.0 SENSITIVITY ANALYSES

Some sensitivity analyses were carried out for the default shape to identify the leverage of various variables on the availability and performance of stratosphere airship. The results of these sensitivity analyses are discussed as follows.

Figure 7 shows the effect of altitude on airship length for wind speed profile data. Lowest length is expected at 19km altitude. The reason is that as the altitude of operation is increased, the loss in buoyancy results in lower lift, and hence for a given payload, the required envelope volume is increased corresponding to the increase of airship length. At lower altitudes, lift is higher; however, the increase in drag leads to more power and energy to meet the station-keeping requirement, which causes the increase of the area of solar cell and the weight of fuel cell corresponding to larger airship length. For the given operating conditions, the minimum airship length for the case was seen to occur at an operating altitude of 19km.

https://doi.org/10.1017/S0001924000003183 Published online by Cambridge University Press

Table 6
Key input parameters and results of the conceptual design using AODAP

	Default Shape	Minimum Drag	Composite Objective
Altitude	20,000m	20,000m	20,000m
Weight of payload	1,000kg	1,000kg	1,000kg
Power of payload	10kW	10kW	10kW
Max design speed	25ms^{-1}	25ms^{-1}	25ms^{-1}
Airship length	194m	226m	166m
Design volume	235,144m^3	249,106m^3	228,713m^3
Envelope area	23,280m^2	25,812m^2	21,782m^2
Area of solar array	10,578m^2	10,830m^2	10,775m^2
Maximum diameter	50·08m	47·10m	51·52m
CDV of envelope	0·023779	0·023501	0·024734
Structure weight	9,845·06kg	10,693·60kg	9,372·54kg
Energy weight	5,138·73kg	5,251·28kg	5,226·51kg
Other weight	718·48kg	810·63kg	661·80kg
Payload weight	1,000kg	1,000kg	1,000kg
Total weight	16,702·27kg	17,755·51kg	16,260·85kg

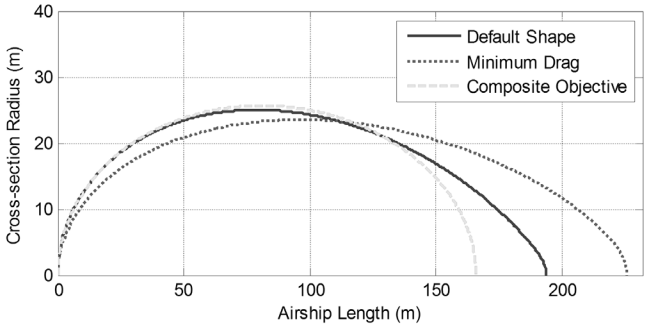


Figure 6. Shape comparisons of various designs.

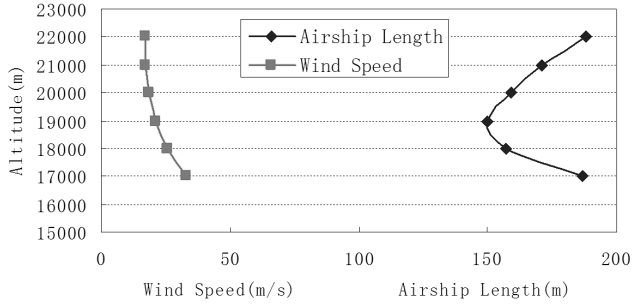


Figure 7. Optimum altitude as indicated by the airship length with wind speed profile data.

Figure 8 shows that the airship length increases almost linearly in proportion to the area density of envelope fabric. As the area density of envelope fabric is increased from 0·162kg/m^2 to 0·256kg/m^2, the required airship length increases from 172m to 193m.

Figure 9 shows that the airship length increases almost linearly in proportion to the area density of solar cell. As the area density of solar cell is increased from 0·1575kg/m^2 to 0·2625kg/m^2, the required airship length increases from 176m to 184m.

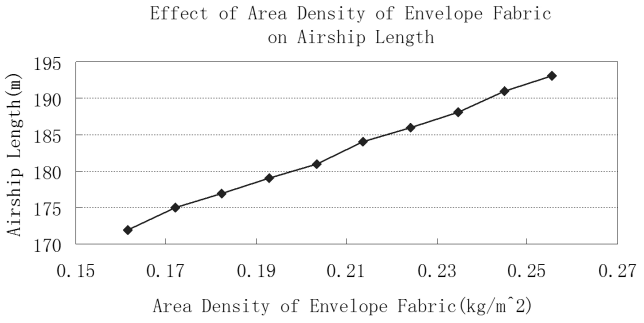


Figure 8. Effect of area density of envelope on airship length.

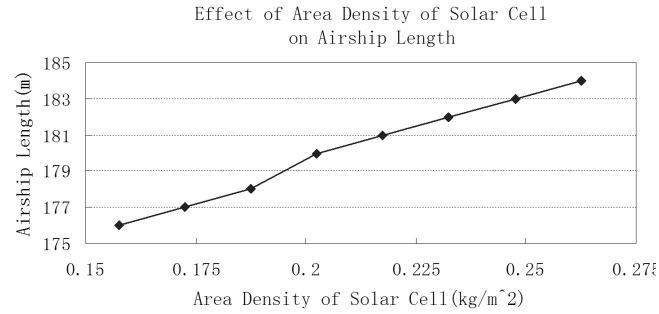


Figure 9. Effect of area density of solar cell on airship length.

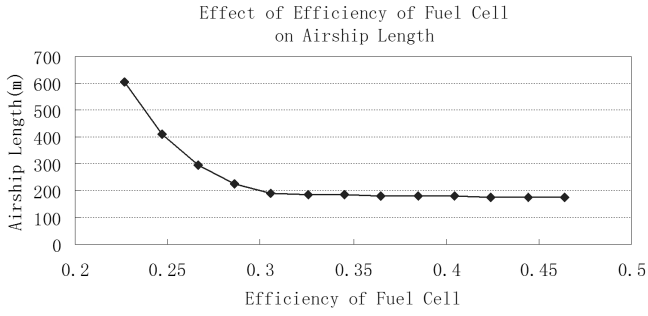


Figure 10. Effect of efficiency of fuel cell on airship length.

Figure 10 shows that the airship length decreases almost linearly in inverse proportion to the efficiency of fuel cell when the latter one is higher than a certain value called a turning point. When the efficiency of fuel cell is lower than the value of the turning point, the airship length will decreases exponentially in inverse proportion to it. The value of the turning point is around 0·3.

Figure 11 shows that the relationship between the airship length and the efficiency of solar cell is similar to the relationship between the airship length and the efficiency of fuel cell. When the efficiency of solar cell is lower than the value of the turning point, the airship length will decrease exponentially in inverse proportion to it; otherwise the airship length will decrease almost linearly in inverse proportion to it. The value of the turning point is around 0·08.

https://doi.org/10.1017/S0001924000003183 Published online by Cambridge University Press

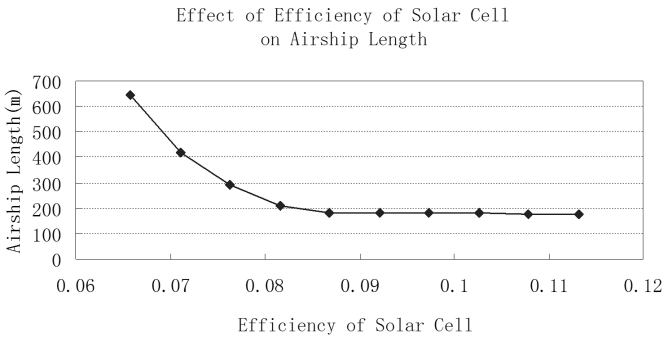


Figure 11. Effect of efficiency of solar cell on airship length.

9.0 CONCLUSIONS

Our methodology for optimisation design and analysis of stratosphere airship is quite useful for carrying out the conceptual design studies to get an estimate of the size and weight of various components or sub-systems, and to study the sensitivity analyses. Furthermore, the codes of the AODAP platform are open-ended, so it can be upgrade easily when some more accurate information becomes available. Finally, a summary of the conclusions and recommendations are enumerated as follows.

1. AODAP presents a valid methodology to obtain the baseline specifications of an airship during the phrase of conceptual design. Optimisation was introduced into the procedure of design and the MDO was integrated into the composite objective, which makes AODAP different from previous methodologies and codes.
2. AODAP was validated using parameters from HALE prototype design and the HI-SPOT conceptual design. The results of the AODAP show reasonable agreement with the reference design. The versatility of the AODAP code also allows a wide range of studies to be performed for a variety of feasible concepts. Furthermore, the AODAP was also validated by the design of the Goodyear Blimp, which verifies that our methodology can also apply to the low altitude airship.
3. AODAP was used with wind speed profile data to identify an optimum operating altitude near 19km.
4. AODAP showed that the length of airship increases almost linearly in proportion with the area density of envelope and the area density of solar cell respectively and the length of airship decreases because of the increase of the efficiency of fuel cell and solar cell. So the development of lighter components and more efficient fuel cells and solar cells would increase the feasibility designs of stratosphere airship by decreasing the required volume and length of airship.
5. AODAP also proved that it is significant to improve when the efficiencies are under the values of the turning points. But it is not worthy of improving the efficiency when the efficiencies reach some certain values. The values of the turning points of the fuel cell and solar cell are 0·3 and 0·08 respectively for the default shape.

ACKNOWLEDGEMENTS

This work was supported by the National Hi-Tech Research and Development Program (863) of China under Grant No 2007AA705003.

REFERENCES

1. COLOZZA, A. and DOLCE, J.L. High-altitude, long-endurance airships for coastal surveillance, 2005, NASAPTM-2005-213427.
2. OZOROSKI, T.A., MAS, K.G. and HAHN, A.S. A PC-based design and analysis system for lighter-than-air unmanned vehicles, 2003, 2nd AIAA 'Unmanned Unlimited' System, Technologies, and Operation-Aerospace', San Diego, California.
3. PANT, R.S. A methodology for determination of baseline specifications of a non-rigid airship, 2003, AIAA's 3rd Annual Aviation Technology, Integration, and Operation (ATIO) Tech, Denver, Colorado.
4. Engineering Science Data, October 1977, 77021, Properties of a Standard Atmosphere.
5. KHOURY, G.A. and GILLETT, J.D. *Airship Technology*, 1999, Cambridge University Press, Cambridge.
6. NATIO, H., EGUCHI, K. and HOHSINO, T. ET AL. Design concept and analysis of solar power subsystem for SPF airship operation, 1999, AIAA 99-3913.
7. INGBER, L. Adaptive simulated annealing (ASA), 1993, Global optimisation C-code, http://www.ingber.com/#ASA?CODE, Caltech Alumni Association, Pasadena, California.
8. DEB, K., PRATAP, A., AGARWAL, S. and MEYARIVAN T. A Fast and elitist multi-objective genetic algorithm: NSGA-II, *IEEE Transactions on Evolutionary Computation*, 2002, **6**, (2), pp 182-197.
9. SCHITTKOWSKI, K. NLPQL: A Fortran subroutine for solving constrained nonlinear programming problems, *Annals of Operations Research*, 1985/86, **5**, pp 485-500.
10. HALE Specifications. www.lindstrand.co.uk.
11. HI-SPOT Conceptual Design Study Final Report, Lockheed Missiles and Space, N62269-81-C-0276, March 1982.
12. Goodyear Blimp Technical Statistics, www.goodyearblimp.com.

https://doi.org/10.1017/S0001924000003183 Published online by Cambridge University Press